Sound & Vibration 2024, 59(1), 1765.
https://doi.org/10.59400/sv1765

Article

Finite element modeling and vibration control of composite beams with partially covered active constrained layer damping

Zhicheng Huang*, Yang Li, Yang Cheng, Xingguo Wang

College of Mechanical and Electronic Engineering, Jingdezhen Ceramic University, Jingdezhen 333001, China
* **Corresponding author:** Zhicheng Huang, huangzhicheng@jci.edu.cn

CITATION

Huang Z, Li Y, Cheng Y, Wang X. Finite element modeling and vibration control of composite beams with partially covered active constrained layer damping. Sound & Vibration. 2024; 59(1): 1765. https://doi.org/10.59400/sv1765

ARTICLE INFO

Received: 23 September 2024
Accepted: 10 October 2024
Available online: 15 November 2024

Abstract: This paper analyzes the active vibration control of sandwich beams using Active Constrained Layer Damping (ACLD). The finite element model of the viscoelastic sandwich beam combines finite element method with the Golla Hughes McTavish (GHM) model, using a 2-node 8 degrees freedom element. The finite element model is validated by the first four natural frequencies of the model in the literature, and the governing equations of sandwich beams are generated based on the Hamiltonian principle. The physical space dynamic condensation technique and state space complex mode decoupling method are employed to reduce the order of the structural model. This is necessary because free degree of the finite element model is too high to directly control the structure's vibration. It shows that the fundamental physical characteristics of the structure may remain largely unchanged while the physical and state spaces are jointly reduced. We investigated how the positions and coverages of ACLD patches impact on the active control, vibration damping of viscoelastic sandwich beams.

Keywords: active vibration control; finite element method; viscoelastic materials; partially covered Active Constrained Layer Damping (ACLD); dynamic condensation; sandwich beams

1. Introduction

Thin-walled constructions are employed increasingly often in aircraft engineering and vehicle production as science and technology advance. Even if the vibration frequency is near to the natural frequency, the thin-walled structure will vibrate due to its small mass and thickness when subjected to external pressures. The ACLD-treated sandwich structure based on active damping has excellent vibration resistance. The composite structure includes a piezoelectric layer, a base layer and a viscoelastic material. It has the characteristics of light weight, high rigidity, strong driving ability and excellent vibration damping performance.

Numerous researchers have studied and used the active constrained layer damping (ACLD) method on structures since the early 1990s. The function as both sensors and actuators is a distinctive characteristic of piezoelectric materials. The ACLD can increase the shear stress of the viscoelastic layer and overcome the limitations of Passive Constrained Layer Damping (PCLD) [1,2] when utilized as an actuator and in accordance with a suitable control law [3,4].

ACLD treatment in sandwich structures can be achieved by combining the active capabilities of piezoelectric materials at low frequencies with the strong ability of passive viscoelastic materials to dissipate vibrational energy at high frequencies. Abhay Gupta et al. [5] added solid particles to the viscoelastic layer of a sandwich conveyor to improve damping and reduce the vibration amplitude of the structure.

Yongbin Guo et al. [6] described the modal frequencies and damping behavior of ACLD-treated beam structures when parameters such as temperature and angular velocity were varied. Mevada et al. [7] studied active damping temperature control in sandwich support structures , and conclude that ACLD patches have a better damping effect on low-temperature structures. Khizar Hayat et al. [8] Introduced a multi-step damage identification process, and provided a comprehensive method for structural health monitoring of different structures through vibration analysis. Diyar Khan and Rafal burdzik [9] reviewed the measurement and analysis parameters, methods and standards, prediction and control measures of traffic vibration and noise in many countries.

At the beginning of the 21st century, the finite element method of sandwich structure has been widely accepted. AH Sheikh et al. [10] proposed a finite element model representing the structure and potential of thin-walled smart laminated composite plate. So Shi et al. [11] combined the GHM model and finite element model, and proposed a finite element model method for active vibration control of ACLD elements. SG Wong et al. [12] conducted a vibration analysis of the forced vibration of sandwich beams using a finite element model of beam elements with 1-node 6 degrees. A.R. Daman pack et al. [13,14] proposed a sandwich beam finite element with18 mechanics and potential degrees of freedom physical nodes, at the same time, a sandwich beam element for analyzing the flexible core and delaminated regions is proposed. Based on the shear stress and compression damping mechanism, Huang et al. [14,15] respectively developed two kinds of finite element models of viscoelastic sandwich structures, which further improved the accuracy of the model. Zhicheng Huang et al. [16] Established the integral finite element model of elastic viscoelastic elastic sandwich beam structure based on two damping mechanisms. Gradually, a growing number of scientists are working on the active damping of vibrations in sandwich structures. Lu Qifa et al. [17] studied the low-frequency vibration of composite sandwich beams by experiments and simulations, and adopted the adaptive method to control the vibration of sandwich beams.

After comparing numerous references, it is found that the full-coverage ACLD patch is often not the best way. Li Fengming et al. [18] showed that in an active control analysis of the sandwich beam, a beam with two ACLD patches had better active control than with one ACLD patch. LiangLi et al. [19] analyzed the free vibration of a fully covered ACLD composite plate and studied the control parameters. H. Zheng et al. [20] examined the damping analysis of a simply-supported beam by dividing the CLD patches into various lengths and distances. L.Zoghaib et al. [21] conducted a structurally damped vibration analysis at the CLD patch position and showed that the patch position plays a less important role in the higher frequency range or larger patch size. The findings of Yaman M. et al. [22] showed that the best vibration reduction effect was obtained when the CLD patch was covered by 50%. Navin Kumar et al. [4] studied the effect of ACLD patch coverage on the dissipation factor, and concluded that when the patch coverage reaches 50%, the beam treated by ACLD can obtain the first-order modal maximum. Y.S. Gao et al. [23] indicated that the loss factor also decreases with the decrease of the coverage of CLD patches, but the natural frequency is opposite.

Most researchers currently typically focus on full coverage ACLD patches and rarely use partial coverage. The latter group analyses a structure's passive properties the most, while the pieces that actively control vibration are much rarer. In order to address these shortcomings, this study bases its finite element code for ACLD sandwich beams on the Hamiltonian principle and is written in MATLAB. Active vibration control of laminated beams by varying the length and position of the overlaying ACLD patches, and comparing the effects of different structures on the effectiveness of active control. Among them, the Linear Quadratic Regulator (LQR) is a control method suitable for state-space forms, capable of considering multiple performance metrics and system robustness simultaneously. Therefore, LQR is used as a controller.

This paper evaluates the model in fields such as airplanes and automobiles, comparing the performance differences between active vibration control and traditional passive vibration control systems. Additionally, it studies how to divide active damping patches to enhance vibration reduction effectiveness. This research results an innovative and efficient vibration control scheme for the aerospace and automotive fields, along with theoretical and practical references for the application of active damping structures. The remainder of the paper is organized as follows: Section 2 finite element model downscaling, Section 3 model validation and numerical analysis, Section 4 effect of different ACLD patch positions and lengths on active control of vibration, and Section 5 provides conclusions.

2. Finite element modeling of damped sandwich beams

2.1. Basic assumptions of the model

(1) Due to the high elastic modulus of the base beam and the piezoelectric layer relative to the viscoelastic layer, the base beam and the piezoelectric layer can be considered as Euler-Bernoulli beams;
(2) Perfect bonding is assumed between layers, ensuring no relative displacement between the layers;
(3) The density of each material layer is uniform and complies with the basic assumptions of material mechanics;
(4) Due to the large beam aspect ratio, the effect of rotational inertia of each layer is ignored to simplify the analysis and improve the computational efficiency;
(5) The viscoelastic material properties are characterized using the GHM model, which simulates hysteretic damping by adding dissipative coordinates, and viscoelastic damping coefficients are discussed only in Maxwell's linear theory of viscoelasticity;
(6) The voltage is uniformly distributed over the entire surface of the piezoelectric layer, producing a uniform electric field, and the electric pressure applied to the damped sandwich beam is uniformly distributed over the element.

2.2. Shape function of Active Constrained Layer Damping (ACLD) beam

As shown in **Figure 1**, the ACLD element is a two-node composite three-layer beam element, which is composed of a piezoelectric layer, viscoelastic layer and base

beam layer from top to bottom. According to the overall structure of the laminated beam, it is divided into several 2-node beam elements. Considering the boundary conditions, the appropriate number of nodes and element lengths are selected, and the finite element mesh of the whole beam structure is obtained after assembly.

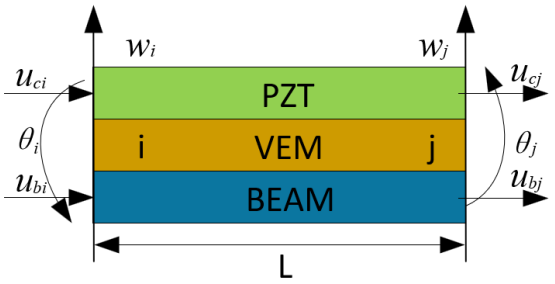

Figure 1. 2-node 8 degrees of freedom (DOF) sandwich beam elements.

The displacement vector of ACLD elements is given by:

$$\{V^e\} = \{w_i \ \theta_i \ \ u_{bi} \ u_{ci} \ w_j \ \theta_j \ \ u_{bj} \ u_{cj}\}^T \tag{1}$$

The nodal displacements in the ACLD element can be represented by interpolation functions *N*. These shape functions are derived using standard finite element interpolation techniques for beam elements:

$$\{V^e\} = [\omega \ \theta \ u_b \ u_c]^T = N\{V^e\} \tag{2}$$

where $N = [N_\omega \ N_\theta \ N_{ub} \ N_{uc}]^T$ .The finite element shape functions of transverse displacement, axial displacement of foundation beam and axial displacement of PZT layer are respectively:

$$\omega = [N_\omega]\{V^{(e)}\} \ \theta = [N_\theta]\{V^{(e)}\} \ u_b = [N_{ub}]\{V^{(e)}\} \ u_c = [N_{uc}]\{V^{(e)}\} \tag{3}$$

$N = [N_\omega \ N_\theta \ N_{ub} \ N_{uc}]^T$ in the above equation corresponds to the four shape function matrices of the unit, denoted respectively:

$$\begin{aligned}
N_\omega &= [1 - 3(\frac{x}{l})^2 + 2(\frac{x}{l})^3 \ \text{x-}2(\frac{x}{l})^2 + \frac{x^3}{l^2} \ \ 0 \ \ 0 \ \ 3(\frac{x}{l})^2\text{-}2(\frac{x}{l})^3 \ \text{-}\frac{x^2}{l} + \frac{x^3}{l^2} \ \ 0 \ \ 0] \\
N_\theta &= [-6(\frac{x}{l^2}) + 6(\frac{x^2}{l^3}) \ \ 1\text{-}4(\frac{x}{l}) + 3(\frac{x}{l})^2 \ \ 0 \ \ 0 \ \ 6x(1\text{-}\frac{x}{l}) \ \ \text{-}2(\frac{x}{l}) + 3(\frac{x}{l})^3 \ \ 0 \ \ 0] \\
N_{ub} &= [0 \ \ 0 \ \ 0 \ \ 1\text{-}\frac{x}{l} \ \ 0 \ \ 0 \ \ 0 \ \ \frac{x}{l}] \\
N_{uc} &= [0 \ \ 0 \ \ 0 \ \ 1\text{-}\frac{x}{l} \ \ 0 \ \ 0 \ \ 0 \ \ \frac{x}{l}]
\end{aligned} \tag{4}$$

The dynamic relationship between the PZT layer and the base beam layer is shown in **Figure 2**. According to the first-order shear deformation theory, the expressions for the longitudinal displacement u_v and shear strain γ of the viscoelastic layer can be deduced as:

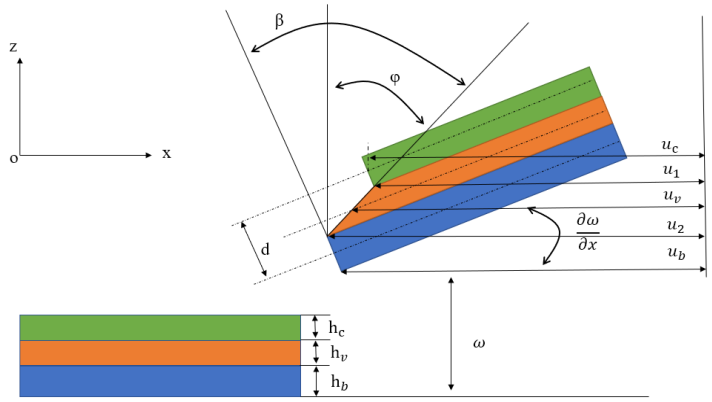

Figure 2. The geometry and deformation of ACLD beam left: Before deformation; right: After deformation.

$$d = \frac{1}{2}(h_c + h_b) + h_v \tag{5}$$

$$u_v = \frac{1}{2}[u_c + u_b] + (\frac{h_c - h_b}{2})\frac{\partial\omega}{\partial x}] \tag{6}$$

$$\gamma = \frac{1}{h_v}[(u_c - u_b) + d\frac{\partial\omega}{\partial x}] \tag{7}$$

From the geometry and deformation of ACLD beam. Where ∂ω/∂x is the cross-section rotation of ACLD beam; φ is the shear angle of Viscoelastic layer; γ indicate the shear strain of Viscoelastic layer; u_c , u_b respectively the transverse displacement in PZT layer and base beam layer. The thickness of the PZT layer, the viscoelastic layer and the base beam are h_c, h_b and h_v , respectively.

The constitutive equation of a piezoelectric layer in a sandwich beam is presented here.

$$\begin{bmatrix}\varepsilon \\ D\end{bmatrix} = \begin{bmatrix}S_{11}^{E} & d_{31} \\ d_{31} & \varepsilon_{33}^{\tau}\end{bmatrix}\begin{bmatrix}\tau \\ E\end{bmatrix} \tag{8}$$

where ε is the mechanical strain in the axial direction; S_{11}^{E} is the elastic compliance constant; d_{31} is the piezoelectric constant; E is the electric field intensity, D is the electric displacement, τ is the transverse mechanical traction, ε_{33}^{τ} is the dielectric constant.

2.3. GHM model

The GHM model is frequently utilized to represent the complicated variable modulus model in the finite element analysis of viscoelastic materials. The dissipative coordinates used in the GHM method allow the consideration of viscoelastic damping effects without the constraints of steady state motion. The viscoelastic material properties in the GHM model can respond to frequency and temperature changes more accurately.

In the GHM model, the composite shear modulus of viscoelastic materials is expressed by the micro vibrator model. The micro vibrator model represents the complex shear modulus function sG(s) of materials by a series of micro vibration terms.

where sG(s) is given by [24]:

$$\mathrm{sG}(s)=\mathrm{G}^{\infty}[1+\sum_{k=1}^{N}\alpha_k\frac{s^2+2\hat{\xi}_k\hat{\omega}_k s}{s^2+2\hat{\xi}_k\hat{\omega}_{\ k}s+\hat{\omega}_k{}^2}] \tag{9}$$

where G^{∞} is the steady-state value of the relaxation characteristic under the condition of time $t=\infty$, specifically the final value of the shear modulus of viscoelastic materials, s is the Laplace operator, $\{\alpha_k,\ \hat{\omega}_k,\ \hat{\xi}_k\}$ are three groups of ordinary numbers. It determines the affect on every micro vibrator. It additionally determines the complicated shear modulus function of viscoelastic materials in the pull domain. When the micro vibrator term reaches order k, then the number of parameters to be determined is $3k+1$. The GHM model performs well in describing the properties of viscoelastic materials, and therefore it has been widely used in the description of dynamic response and vibration characteristics.

The time domain expression of the viscoelastic sandwich beam dynamic model is:

$$\widetilde{M}\ddot{q}+\widetilde{D}\dot{q}+\widetilde{K}q=\tilde{f} \tag{10}$$

where

$$\widetilde{M}=\begin{bmatrix} M^e & 0 & \cdots & 0 \\ 0 & \frac{\alpha_1}{\hat{\omega}_1^2}\Delta & 0 & \vdots \\ \vdots & 0 & \ddots & 0 \\ 0 & \cdots & 0 & \frac{\alpha_N}{\hat{\omega}_N^2}\Delta \end{bmatrix} \tag{11}$$

$$\widetilde{D}=\begin{bmatrix} 0 & 0 & \cdots & 0 \\ 0 & 2\hat{\xi}_1\frac{\alpha_1}{\hat{\omega}_1}\Delta & 0 & \vdots \\ \vdots & 0 & \ddots & 0 \\ 0 & \cdots & 0 & 2\hat{\xi}_N\frac{\alpha_N}{\hat{\omega}_N}\Delta \end{bmatrix} \tag{12}$$

$$\widetilde{K}=\begin{bmatrix} K_e+\tilde{k}(1+\sum_{K=1}^{N}\alpha_k) & -\alpha_1 R & \cdots & -\alpha_N R \\ -\alpha_1 R^T & \alpha_1\Delta & 0 & 0 \\ \vdots & 0 & \ddots & 0 \\ -\alpha_N R^T & 0 & 0 & \alpha_N\Delta \end{bmatrix} \tag{13}$$

$$q=\begin{Bmatrix} x \\ Z_1 \\ \vdots \\ Z_N \end{Bmatrix},\ \tilde{f}=\begin{Bmatrix} f_e \\ 0 \\ 0 \\ 0 \end{Bmatrix} \tag{14}$$

The dynamic finite element equation of viscoelastic sandwich beam can be obtained by assembling the elements as follows:

$$M\ddot{q} + D\dot{q} + Kq = f \tag{15}$$

where M is the total mass matrix of structure; D is the total damping matrix of structure; K is the total stiffness matrix of structure, and f is the sum of external incentives to the structure.

The derived equation for the natural frequency of a cantilever beam is:

$$f_n = \frac{\sqrt{D_m}}{2\pi} \tag{16}$$

$$K \times V_m = M \times V_m \times D_m \tag{17}$$

where D_m and V_m are eigenvalues and eigenvectors of K and M, and fulfills the Equation (17).

3. FE model reduction

The order of the structural finite element model system is excessively high due to the GHM model's large number of dissipative degrees of freedom, making the system unobservable and uncontrollable. The control effectiveness may decrease or become uncontrollable. As a result, the order of the dimensions of the model desires to be reduced.

3.1. Dynamic condensation in physical space

The z direction displacement of the x and y direction linear displacement of the constraint layer in the structure of the ACLD element is taken as the primary degree of freedom [25], and other physical degrees of freedom and dissipative degrees of freedom are taken as the secondary degrees of freedom.

where Equation (15) can be written as：

$$\begin{bmatrix} M_{mm} & M_{ms} \\ M_{sm} & M_{ss} \end{bmatrix} \begin{Bmatrix} \ddot{X}_m(s) \\ \ddot{X}_s(s) \end{Bmatrix} + \begin{bmatrix} D_{mm} & D_{ms} \\ D_{sm} & D_{ss} \end{bmatrix} \begin{Bmatrix} \dot{X}_m(s) \\ \dot{X}_s(s) \end{Bmatrix} + \begin{bmatrix} K_{mm} & K_{ms} \\ K_{sm} & K_{ss} \end{bmatrix} \begin{Bmatrix} X_m(s) \\ X_s(s) \end{Bmatrix} = \begin{Bmatrix} F_m(s) \\ F_s(s) \end{Bmatrix} \tag{18}$$

The dynamic condensation matrix E between the primary and secondary degrees of freedom of ACLD element structure is：

$$E = K_{ss}^{-1}[(M_{ss} + M_{ss}R)M_E^{-1}K_E - K_{sm}] \tag{19}$$

The kinetic equation after polycondensation is：

$$M_E^{(i)}\ddot{X}_m + D_E^{(i)}\dot{X}_m + K_E^{(i)}X_m = F_E^{(i)} \tag{20}$$

3.2. The model reduction process in state space

Even if physical space order is reduced, the systematic dimensions are still too much for the controller design. Therefore, it is still essential to lower the model's

order, remove the unobservable and uncontrollable degrees of freedom from the system, and decrease the model's size.

Because the complex mode truncation method can supply a steady skill of order reduction, and the modal system is extra fine at each resonant frequency [26], it can completely abandon the unobservable and uncontrollable dimensions in the model, and has a broad variety of applications.

Decoupling and truncation of complex modes in the state space

Introducing auxiliary equation$M_E\dot{X} - M_E\dot{X} = [0]$ into Equation (20).

The sandwich structure system model can be expressed as：

$$\begin{Bmatrix}\ddot{X}\\ \dot{X}\end{Bmatrix} = \begin{bmatrix}0 & M_E\\ M_E & D_E\end{bmatrix}^{-1}\begin{bmatrix}M_E & 0\\ 0 & -K_E\end{bmatrix}\begin{Bmatrix}\dot{X}\\ X\end{Bmatrix} + \begin{bmatrix}0 & M_E\\ M_E & D_E\end{bmatrix}^{-1}\begin{Bmatrix}F_E\\ 0\end{Bmatrix} + \begin{bmatrix}0 & M_E\\ M_E & D_E\end{bmatrix}^{-1}\begin{Bmatrix}F_E\\ 0\end{Bmatrix} \tag{21}$$

Equation (21) can be written as：

$$\begin{cases}\dot{Y} = AY + Bf\\ Z = CY\end{cases} \tag{22}$$

where：

$$A = \begin{bmatrix}-M_E^{-1}D_E & -M_E^{-1}K_E\\ 0 & I\end{bmatrix}, B = \begin{bmatrix}M_E^{-1}F_E\\ 0\end{bmatrix}, Y = \begin{bmatrix}\dot{X}\\ X\end{bmatrix} \tag{23}$$

3.3. Active controller design

Viscoelastic materials undergo temperature and frequency-dependent property changes as a result. In dynamic modeling, there are a lot of unknowns regarding the assumptions, models, and order reduction. Because this work uses the finite element approach, physical space, and state space method. A provided system in the state space structure is a LQR controlled object, which offers exceptional comfort for the active control of the system. Multiple indications can be taken into account simultaneously by LQR, which is a developed aspect of the growth of contemporary control theory.

LQR control

LQR (linear quantitative regulator) is shown in **Figure 3**. The optimal control strategy is that the designed state feedback controller should minimize the quadratic objective function *J* [27,28], and the gain *K* is uniquely determined by the weighting matrices Q and R.

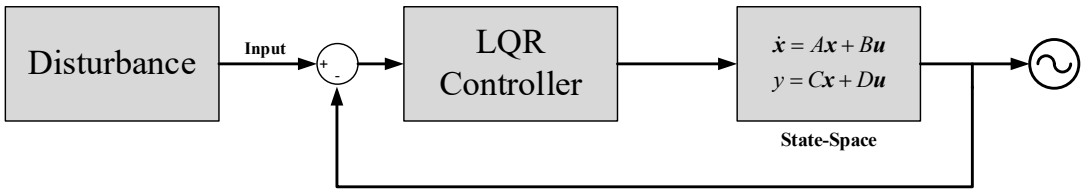

Figure 3. LQR control.

The expression form of common objective function *J* is：

$$J = \int_0^\infty (x^T(t)Qx(t) + u^T(t)Ru(t))dt \tag{24}$$

where the Q and R scalar weighted matrix.

4. Model validation and numerical analysis

In order to demonstrate the accuracy of the vibration dynamic analysis of this structural model under various parameters and to confirm the viability and efficacy of controlling LQR vibration of sandwich structures and ACLD element placed at various locations, the vibration of sandwich beams with various geometric parameters, such as placement position and length, are each individually analyzed in this chapter. The control objective is to investigate the free vibration displacement response of viscoelastic sandwich beams with fixed-free boundary conditions.

4.1. Model validation

In order to verify the accuracy of the model, this paper adopts a 2-node 8 degrees freedom element model with the clamped-free boundary. The position of the partial coverage patch of the ACLD element is shown in **Figure 4**. The vibration analysis of the sandwich beam is carried out based on the method in this paper and the natural frequencies of the ACLD cantilever beam in the comparative literature to verify the accuracy of the model.

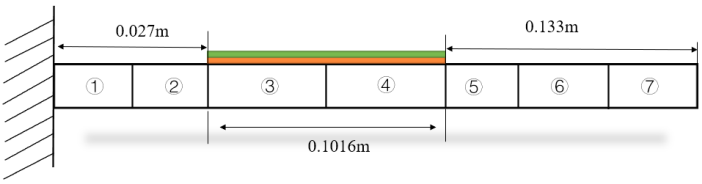

Figure 4. Viscoelastic sandwich cantilever beam.

The model example is an ACLD cantilever beam, **Table 1** shows specific material parameters. **Table 2** compares the natural frequencies in this method and literature. For the calculation of the first four natural frequencies of the sandwich structure with the boundary condition clamped-free, the error range difference obtained by the method in this paper is 0.25%–3.21% so the finite element model in this paper has good accuracy.

Table 1. Material and geometrical properties of ACLD beam.

	Base beam	**layer PZT layer**	**VEM layer**
length (m)	0.35	0.35	0.35
width (m)	0.015	0.015	0.015
thickness (m)	0.002286	0.000762	0.00025
density (kg)	7600	7600	1250
Elastic modulus (Gpa)	7.4×10^{10}	6.67×10^{10}	
Poisson ratio	0.3	0.3	0.3

Table 1. (*Continued*).

	Base beam	layer PZT layer	VEM layer
Piezoelectric constant (m/V)		-1.75×10^{10}	
G^{∞}			5×10^5 Pa
α			6.0
ς			4.0
ω			10000rad/s

Table 2. Frequencies of the four first modes for ACLD cantilever beam.

The modal	[9]	this paper	Error(%)
1 mode	27.90	27.83	0.25%
2 mode	150.12	147.83	1.52%
3 mode	442.97	429.66	3.00%
4 mode	831.76	805.08	3.21%

4.2. Model reduction

With **Table 1** as the structural parameters, the clamped-free boundary sandwich beam model is obtained by using the finite element method. The physical space dimension is 54 × 54, and the state space dimension is 108 × 108. Before designing the controller, the order of the model must be reduced, and the reduced range must conform to the characteristics of system observability and controllability.

Table 3 compares the model's natural frequencies before and after the order reduction. Naturally, the model's natural frequency is essentially unchanged between before and after order reduction. The minimum and highest mistakes among them are 0 and 0.056%. It shows that the structure's physical characteristics are correctly reflected following order reduction.

Table 3. Model comparison before and after order reduction.

Mode	Before order reduction(Hz)	After order reduction(Hz)	Relative error(%)
1	27.83	27.83	0.0
2	147.83	147.85	0.013
3	429.66	429.78	0.028
4	805.08	805.53	0.056

Figure 5 shows how the model's frequency coincidence accuracy is high both before and after the decrease of physical space. Additionally, it demonstrates that the system's accuracy has increased as a result of the addition of complicated mode. The control system can still be observed, controlled, and maintained accurately after the state space reduction. Each mode is a separate genuine mode that can be used directly in the construction of an active controller.

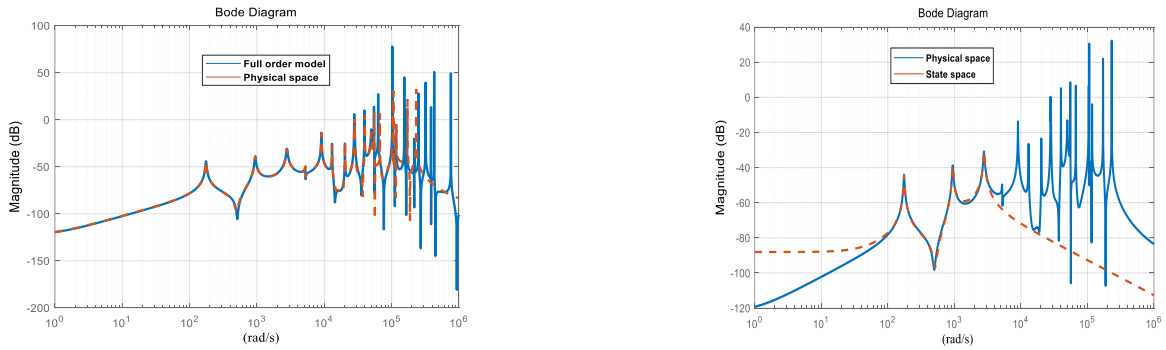

(a) **(b)**

Figure 5. (a) Model reduction in physical space; **(b)** Model reduction in state space (—reduce order model, —full order model).

5. Effect of different ACLD patch placement and length on active vibration control

The content of this chapter is to study the influence of the ACLD patch position and length of sandwich beams on the LQR control of the first three modes. The boundary condition is still clamped-free. The parameter sets the length of the foundation beam of **Table 1** as 0.45m. Other characteristics do not vary, only the length of the piezoelectric and viscoelastic layers are affected by the construction.

5.1. Effect of different positions of ACLD patch on vibration

In this paper, the sandwich beam structure of ACLD patches at six different positions is shown in **Figure 6** from (1) to (6). (1) and (6) ACLD patches are respectively arranged at the clamped end and the free end, and the rest (2) to (5) are arranged at 1/7, 2/7, 3/7, 4/7 along the *x* direction.

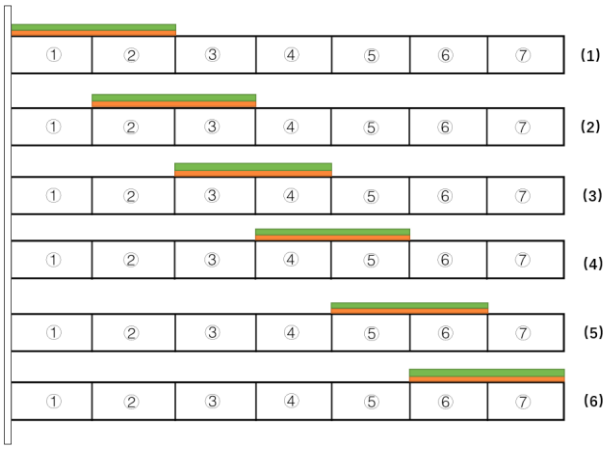

Figure 6. Sandwich beam structures with ACLD arranged in different positions.

The first 6 natural frequencies of each structure in **Figure 6** are calculated for the dynamic analysis of each structure. Because the dynamic properties of the structure can be rather completely described by the first few natural frequencies. The first six natural frequencies of six ACLD placement structures are determined and contrasted

in **Table 1** condition. The modal characteristics of each order are changed according to the change of ACLD patch position and the intrinsic frequency is also changed and the results are shown in **Table 4**. The position of the ACLD patch will alter the stiffness matrix *K* when the total mass is constant. The natural frequency decreases with increasing structural stiffness, and the amount of control force needed for active control increases.

Table 4. First 6 natural frequencies of different structures.

Structure	**Natural frequency （Hz）**					
Mode	(1)	(2)	(3)	(4)	(5)	(6)
1	10.64	9.51	9.08	8.50	7.81	7.08
2	59.98	52.08	50.11	52.39	55.96	53.40
3	150.50	144.07	149.66	152.85	154.41	148.64
4	292.19	287.89	294.98	295.75	298.69	294.63
5	439.11	475.60	429.78	491.96	481.88	494.61
6	590.95	590.89	590.85	590.80	590.75	590.71

Effect of ACLD patch placement on active vibration control

In order to study the influence of ACLD placement on active vibration control, this paper conducts active vibration control on the structures (1)–(6) in **Figure 6**. In this paper, the LQR controller is used to control the free vibration of the sandwich beam. The initial displacement is applied to the structure, and the control parameters are weighted matrix $Q = 1 \times 10^5 I$, $R = 0.5$; Other conditions remain unchanged. The output is the lateral displacement response of the free end of the cantilever beam.

The performance of a structure at passively reducing vibration is shown in **Figure 7** by the amplitude attenuation curves of six uncontrolled constructions. Since the structure of the sandwich beam is clearly recognized to be essentially the same under free vibration, the response convergence of these six constructions is not remarkably different and occurs within 0.5 s. With a vibration attenuation time of 0.115 s and a vibration amplitude of 0.107 meters, structure 6 has the best passive vibration reduction effect. Structure 5 comes in second with a vibration attenuation time of 0.13 s. The structures (3) and (4) perform the poorest in terms of passive vibration reduction. Structure (3)’s attenuation duration is 0.4 s, Structure 4’s maximum beginning amplitude is 0.144 meters, and Structures 1 and 2’s passive vibration reduction performance is average.

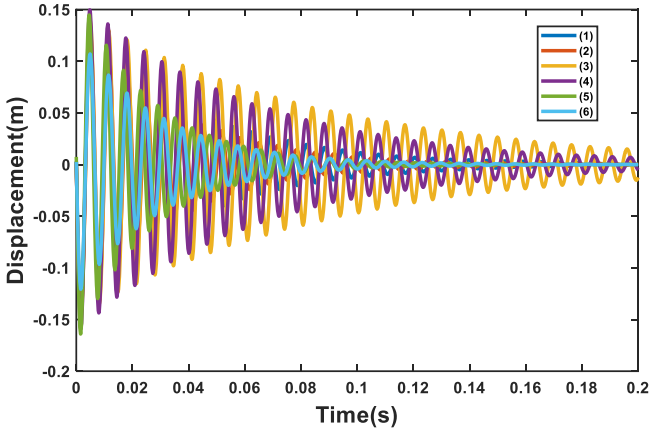

Figure 7. Different structure of sandwich beam amplitude attenuation without control.

The simulation outcomes for active control for various ACLD patch structures are displayed in **Figure 8**. Intuitively, it shows that active control has significantly improved the vibration of the six structures that were the subject of this work. Based on the identical control effect, the active control effect of structure (2) is the best, the vibration reduction effect is extremely significant, the initial amplitude reduction is 44.8% less than the uncontrolled effect, and the vibration attenuation time is 73.3% shorter than the original. Second, compared to structure 2, the effects of structures (1) and (5) on vibration reduction are marginally worse. The peak amplitude and attenuation time are, respectively, 0.1218 m, 0.1003 m, 0.05 s, and 0.043 s. Structures (3) and (6) have a worse impact on vibration reduction than other structures. The results are consistent with the vibration theory and it is evident that the active control performance of the structure with the patch close to the clamped end is marginally better than that of the patch close to the free end. **Table 5** shows the precise vibration values for different structures.

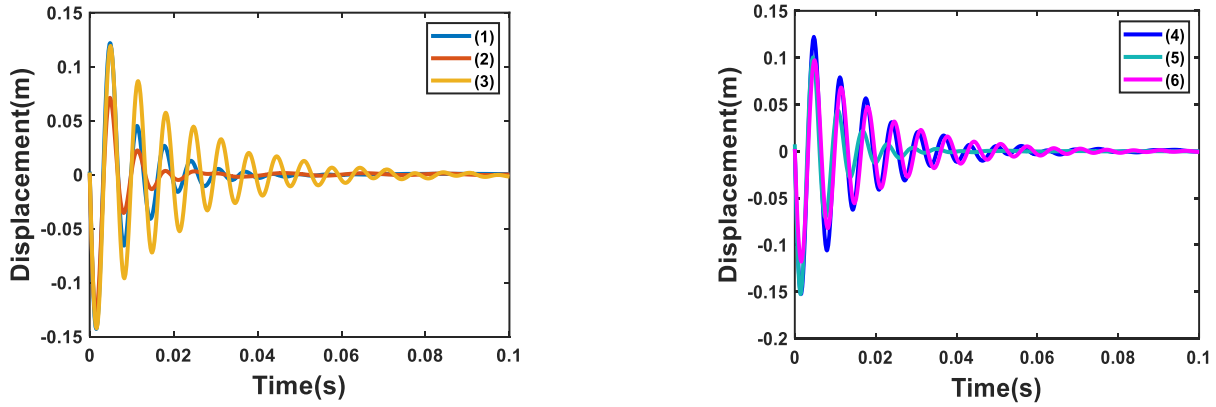

(**a**) (**b**)

Figure 8. Comparisons of amplitude attenuation of different structures with active control. (**a**) Sandwich beam amplitude attenuation of structural (1)–(3); (**b**) Sandwich beam amplitude attenuation of structural(4)–(6).

Table 5. Vibration values of different structures.

	Uncontrol		Active control	
Structure	**Peak amplitude(m)**	**Decay Time(s)**	**Peak amplitude (m)**	**Decay Time (s)**
(1)	0.132m	0.154s	0.122m	0.050s
(2)	0.128m	0.147s	0.071m	0.039s
(3)	0.139m	0.336s	0.119m	0.082s
(4)	0.150m	0.234s	0.122m	0.063s
(5)	0.145m	0.130s	0.100m	0.043s
(6)	0.107m	0.121s	0.096m	0.082s

It may be inferred that the ACLD patch's location within the structure significantly affects the control effect of active vibration control. There is a clear separation between the active control effects associated with various patch placements. Effective and acceptable patch placement can enhance the dampening effect and reduce costs.

5.2. Effect of ACLD patch length on active vibration control

In order to further study the ACLD patch of the sandwich beam, this paper also explored the influence of ACLD patch length on active control. The specific structure is shown in **Figure 9**. The length of the PZT layer and viscoelastic layer gradually increases from 2/7L (0.129m) to L (0.45m). The length of the ACLD element increases by 1/7L each time until it is completely covered. Other parameters are the same as the previous text.

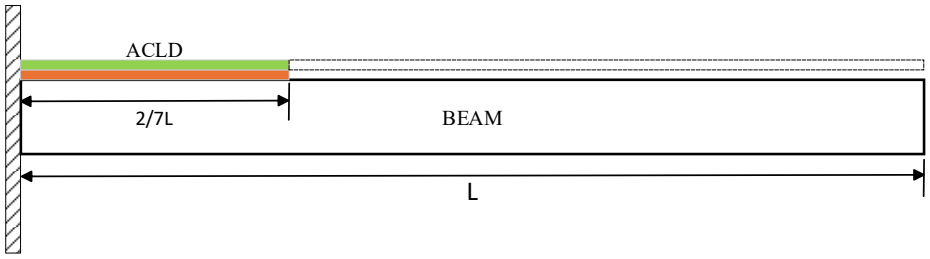

Figure 9. Schematic of cantilever sandwich beam with coverage of ACLD.

Figure 10 shows amplitude attenuation curves of the cantilever ACLD patch from 2/7L to the full without active vibration control. With the ACLD patch from 2/7L to full, the vibration decreases significantly. During the process of patch from 2/7L to 4/7L, the average amplitude attenuation of each 2/7L increase of ACLD patch is 6.5%, and the attenuation time is shortened by 50% on average; The damping effect is slightly lower when the length of the patch is from 4/7L to 5/7L. When the ACLD patch is fully covered, the minimum vibration peak value is 0.0878m, and the attenuation time is also the shortest 0.05s, indicating that the ACLD patch has a very significant effect on the passive vibration reduction performance of sandwich beams.

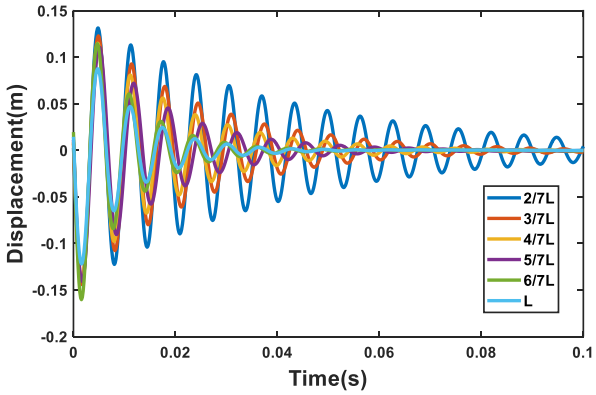

Figure 10. Schematic of cantilever sandwich beam with coverage of ACLD without control.

As for the influence of the length of the ACLD patch on the amplitude of active control, as shown in **Figure 11**, the control parameters are the same as above. It is easy to see the difference between the effect of passive and active control.

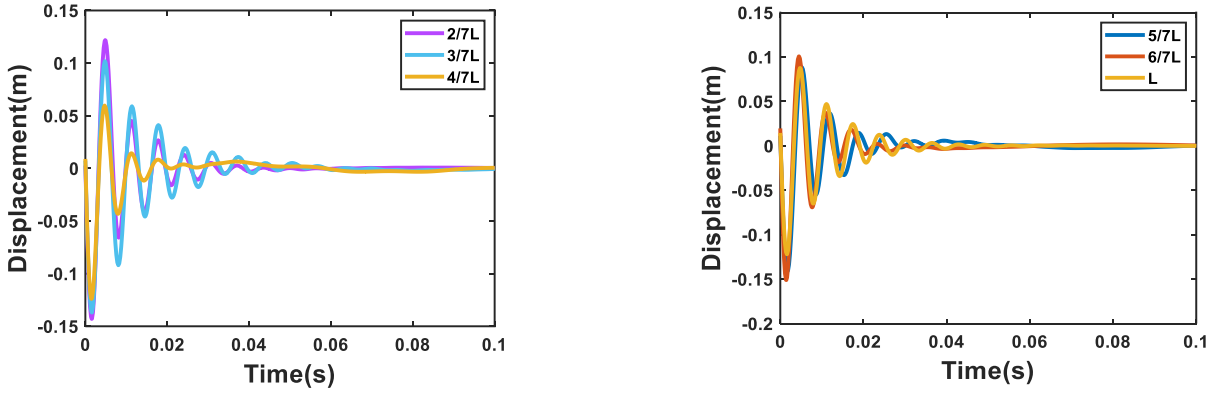

(**a**) (**b**)

Figure 11. Schematic of cantilever sandwich beam with coverage of ACLD with active control; **(a)** Amplitude of the sandwich beam covering 2/7L–4/7L ACLD patch; **(b)** Amplitude of the sandwich beam covering 5/7L–L ACLD patch.

Table 6. Vibration values of different ACLD patch coverage structures.

structures	Uncontrol		Active control	
	Peak amplitude(m)	**Decay Time(s)**	**Peak amplitude (m)**	**Decay Time (s)**
2/7L	0.132m	0.154s	0.122m	0.050s
3/7L	0.123m	0.088s	0.102m	0.058s
4/7L	0.115m	0.086s	0.060m	0.022s
5/7L	0.114m	0.071s	0.089m	0.037s
6/7L	0.114m	0.041s	0.102m	0.028s
L	0.087m	0.044s	0.065m	0.023s

The values in **Table 6** and **Figure 11a** demonstrate that, with the increase in the length of the ACLD patch, it's not that the more patches, the better the active control

effect may be improved. The active control effect of the three structures in **Figure 1b** is slightly worse than that in **Figure 11a**. The vibration attenuation time of the fully covered structure is slightly better than that of the 4/7L patch structure, but the maximum amplitude is 8.9% higher.

It can be shown that the length of the ACLD patch has no absolute influence on active vibration control, the patch coverage rate is close to 50%, and the damping effect is good. Proper patch length can better play the damping performance viscoelastic sandwich, and too long patch may lead to reduced damping effect and even waste of materials. Therefore, specific analysis is required for different engineering problems, and ACLD patches should be arranged reasonably.

6. Conclusions

Based on the first-order shear deformation theory and Hamilton principle, this paper combines the GHM model and the finite element method, generates model of the ACLD cantilever beam. And the order of model is reduced in physical space and state space. LQR is used to control the vibration of the system.

The model's accuracy is confirmed by comparing it to previously published natural frequencies. Analyzed the influence of different patch positions and coverage rates on the vibration of viscoelastic sandwich cantilever beams. Finally, some conclusions are drawn from the current numerical results:

1) The joint order reduction of physical space and state space is accurate and effective. The state space order reduction method can make up for the unobservable and uncontrollable state of the physical model and has a high accuracy for the characteristics of the main modes.
2) The influence of ACLD patches on the vibration of the structure has been greatly improved, whether active or passive, and the different positions of ACLD patches will have a great impact on the natural vibration mode of sandwich beams. With the gradual principle of the patches to move away from the edges, the trend of lower order natural frequencies decreasing is approximately linear. The structure of the patch near the free end has better passive performance but poorer active control of vibration attenuation. The patch is 1/7L from the fixed end for the best active control. The initial peak amplitude of the laminated joint beams was reduced by 44.8% and the vibration decay time was reduced by 73.3% compared to the uncontrolled. In reality, especially in the vibration damping design of aircraft wings, this conclusion provides a reference for quickly finding the optimal control position.
3) When the coverage of the ACLD patch is as large as possible, the passive anti-vibration performance of the sandwich structure is better, and the damping effect gain is lower when the patch is close to full coverage. The results show that among the active controls, the structure with ACLD patch length at 4/7L has the best effect of active control on amplitude attenuation, with 47.8% reduction in maximum amplitude and 74.4% reduction in vibration attenuation time compared to uncontrolled. The active control performance of the structures with patch lengths of 5/7L and 6/7L was slightly lower than that of the full-coverage structures. This finding has important implications for the vibration damping

design for aircraft wings and automobile bodies. Provides a reference for the economics of vibration control systems, reducing materials while still achieving the desired control.

The results show that the finite element model and the reduced order method have good accuracy and effectiveness in predicting the vibration of the ACLD cantilever beam. It can be used to analyze the dynamics of real piezoelectric viscoelastic sandwich structures and active control implementations. However, there are some challenges and limitations of the model, which is not applicable in cases where there are relative displacements between the layers considered. Future research can consider modeling with interlayer displacements for in-depth study, and can also consider improving the algorithm to get better control results. In conclusion, the finite element model of a partially covered actively constrained layer damped laminated beam developed in this paper is instructive for further research.

Author contributions: Writing—review and editing, ZH; funding, ZH; writing-original draft, YC; modeling and simulation, YC; data curation, YL; proofreading of the grammar, XW. All authors have read and agreed to the published version of the manuscript.

Funding: This research was funded by [Natural Science Foundation of China] 11862007, 52265020, [Science and Technology Projects of Jiangxi Education Department of China] GJJ2201027, [Graduate Innovation Special Fund Project of Jingdezhen Ceramic University] JYC202224, JYC202332.

Conflict of interest: The authors declare no conflict of interest.

References

1. Balamurugan, V., Narayanan, S. Finite element formulation and active vibration control study on beams using smart constrained layer damping (SCLD) treatment. Journal of Sound and Vibration, 2002, 249, 227–250
2. Benjeddou, A. Advances in hybrid active-passive vibration and noise control via piezoelectric and viscoelastic constrained layer treatments. Journal of Vibration and Control, 2001, 7, 565–602
3. Gülbahçe, E., Çelik, M. Active vibration control of a smart beam by a tuner-based PID controller. Journal of Low Frequency Noise, Vibration and Active Control, 2018, 37, 1125–1133
4. Kumar, N., Singh, S. P. Vibration and damping characteristics of beams with active constrained layer treatments under parametric variations. Materials & Design, 2009, 30, 4162–4174
5. Gupta, A., Panda, S. Hybrid damping treatment of a layered beam using a particle-filled viscoelastic composite layer. Composite Structures, 2021, 262, 113623
6. Guo, Y., Li, L., Zhang, D. Dynamic modeling and vibration analysis of rotating beams with active constrained layer damping treatment in temperature field. Composite Structures, 2019, 226, 111217
7. Mevada, J. R., Prajapati, J. M. Active vibration control of smart beam under parametric variations. J Braz. Soc. Mech. Sci. Eng., 2018, 40, 394
8. Hayat, K., Mehboob, S., Bux, Q., Ali, A., Matiullab; Khan, D., Altaf, M. Statistical Subspace-Based damage detection and Jerk Energy acceleration for robust structural health monitoring. Buildings, 2023,13,1625
9. Diyar, K., Rafal, B. A review on different regulation for the measurement of transport noise and vibration. Journal of Measurements in Engineering, 2023,11,196-213
10. Sheikh, A. H., Topdar, P., Halder, S. An appropriate FE model for through-thickness variation of displacement and potential in thin/moderately thick smart laminates. Composite Structures, 2001, 51, 401–409
11. Shi, Y. M., Li, Z. F., Hua, H. X., Fu, Z. F., Liu, T. X. The modelling and vibration control of beams with active constrained layer damping. Journal of Sound and Vibration, 2001, 245, 785–800

12. Won, S. G., Bae, S. H., Cho, J. R., Bae, S. R., Jeong, W. B. Three-layered damped beam element for forced vibration analysis of symmetric sandwich structures with a viscoelastic core. Finite Elements in Analysis and Design, 2013, 68, 39–51
13. Damanpack, A. R., Bodaghi, M., Aghdam, M. M., Shakeri, M. Active control of geometrically non-linear transient response of sandwich beams with a flexible core using piezoelectric patches. Composite Structures, 2013, 100, 517–531
14. Damanpack, A. R., Bodaghi, M. A new sandwich element for modeling of partially delaminated sandwich beam structures. Composite Structures, 2021, 256, 113068
15. Huang, Z., Qin, Z., Chu, F. A comparative study of finite element modeling techniques for dynamic analysis of elastic-viscoelastic-elastic sandwich structures. Jnl of Sandwich Structures & Materials, 2016, 18, 531–551
16. Huang, Z., Qin, Z., Chu, F. Damping mechanism of elastic–viscoelastic–elastic sandwich structures. Composite Structures, 2016, 153, 96–107
17. Lu, Q., Wang, P., Liu, C. An analytical and experimental study on adaptive active vibration control of sandwich beam. International Journal of Mechanical Sciences, 2022, 232, 107634
18. Li, F.-M., Kishimoto, K., Wang, Y.-S., Chen, Z.-B., Huang, W.-H. Vibration control of beams with active constrained layer damping. Smart Mater. Struct., 2008, 17, 065036
19. Li, L., Liao, W.-H., Zhang, D., Guo, Y. Vibration analysis of a free moving thin plate with fully covered active constrained layer damping treatment. Composite Structures, 2020, 235, 111742
20. Zheng, H., Tan, X. M., Cai, C. Damping analysis of beams covered with multiple PCLD patches. International Journal of Mechanical Sciences, 2006, 48, 1371–1383
21. Zoghaib, L., Mattei, P.-O. Modeling and optimization of local constraint elastomer treatments for vibration and noise reduction. Journal of Sound and Vibration, 2014, 333, 7109–7124
22. Yaman, M. Finite element vibration analysis of a partially covered cantilever beam with concentrated tip mass. Materials & Design, 2006, 27, 243–250
23. Gao, Y. S., Zhang, S. Q., Zhao, G. Z., Schmidt, R. Numerical modeling for cantilever sandwich smart structures with partially covered constrained viscoelastic layer. Composite Structures, 2022, 281, 114981
24. Zhang, D., Zheng, L. Active vibration control of plate partly treated with ACLD using hybrid control. International Journal of Aerospace Engineering, 2014, 2014, 1–12
25. Huang, Z., Peng, H., Wang, X., Chu, F. Finite element modeling and vibration control of plates with active constrained layer damping treatment. Materials, 2023, 16, 1652
26. Fedotov, A. V. Shape control and modal control strategies for active vibration suppression of a cantilever beam. Lecture Notes in Mechanical Engineering. Springer International Publishing, Cham, 2022, 234–244
27. Mohammed, H. A. U.-Q., Wasmi, H. R. Active vibration control of cantilever beam by using optimal LQR controller. jcoeng, 2018, 24, 1–17
28. Tian, J., Guo, Q., Shi, G. Laminated piezoelectric beam element for dynamic analysis of piezolaminated smart beams and GA-based LQR active vibration control. Composite Structures, 2020, 252, 112480